Figure 3 Erosion rate and cooling-age data. **a**, Plot of [10]Be erosion rate (dots) against distance from the MCT, projected onto a N18°E line. Error bars on the *x* axis represent the projected distance to basin limits; error bars on the *y* axis represent 1σ uncertainty in analytical results. **b**, Plot of [40]Ar–[39]Ar cooling ages (logarithmic scale) against distance from the MCT. Shaded boxes, vertical whiskers, and horizontal lines within boxes represent the interquartile range, limits of analysis results, and median values, respectively. Black dots represent outliers (more than 1.5 times the interquartile range beyond box limits). Widths of boxes represent widths of individual basins. Complete data can be found in ref. 9. Vertical shading and dashed lines show physiographic transition.

Himalayan orogen, so much so that the locus of deep exhumation has been maintained nearly 100 km northwards of the Himalayan thrust front. This focused exhumation sustains the marked topographic front of the high Himalaya, and increases the efficiency of energy dissipation from the Himalayan system. □

1. Cattin, R. & Avouac, J. P. Modeling mountain building and the seismic cycle in the Himalaya of Nepal. *J. Geophys. Res.* **105**, 13389–13407 (2000).
2. Lave, J. & Avouac, J. P. Active folding of fluvial terraces across the Siwaliks Hills, Himalayas of central Nepal. *J. Geophys. Res.* **105**, 5735–5770 (2000).
3. Pandey, M. R., Tandukar, R. P., Avouac, J. P., Lave, J. & Massot, J. P. Interseismic strain accumulation on the Himalayan crustal ramp (Nepal). *Geophys. Res. Lett.* **22**, 751–754 (1995).
4. Jackson, M. & Bilham, R. Constraints on Himalayan deformation inferred from vertical velocity fields in Nepal and Tibet. *J. Geophys. Res.* **99**, 13897–13912 (1994).
5. Bilham, R. *et al.* GPS measurements of present-day convergence across the Nepal Himalaya. *Nature* **386**, 61–64 (1997).
6. Lave, J. & Avouac, J. P. Fluvial incision and tectonic uplift across the Himalayas of central Nepal. *J. Geophys. Res.* **106**, 26561–26591 (2001).
7. Pandey, M. R. *et al.* Seismotectonics of the Nepal Himalaya from a local seismic network. *J. Asian Earth Sci.* **17**, 703–712 (1999).
8. Catlos, E. J. *et al.* Geochronologic and thermobarometric constraints on the evolution of the Main Central Thrust, central Nepal Himalaya. *J. Geophys. Res.* **106**, 16177–16204 (2001).
9. Wobus, C. W., Hodges, K. V. & Whipple, K. X. Has focused denudation sustained active thrusting at the Himalayan topographic front? *Geology* **31**, 861–864 (2003).
10. Hodges, K., Wobus, C., Ruhl, K., Schildgen, T. & Whipple, K. Quaternary deformation, river steepening and heavy precipitation at the front of the Higher Himalayan ranges. *Earth Planet. Sci. Lett.* **220**, 379–389 (2004).
11. Hodges, K. V. Tectonics of the Himalaya and southern Tibet from two perspectives. *GSA Bull.* **112**, 324–350 (2000).
12. DeCelles, P. G. *et al.* Stratigraphy, structure, and tectonic evolution of the Himalayan fold-thrust belt in western Nepal. *Tectonics* **20**, 487–509 (2001).
13. Copeland, P. *et al.* An early Pliocene thermal disturbance of the Main Central Thrust, central Nepal; implications for Himalayan tectonics. *J. Geophys. Res. B* **96**, 8475–8500 (1991).
14. Burbank, D. W. *et al.* Decoupling of erosion and climate in the Himalaya. *Nature* **426**, 652–655 (2003).
15. Bierman, P. R. & Nichols, K. K. Rock to sediment-slope to sea with [10]Be-rates of landscape change. *Annu. Rev. Earth Planet. Sci.* **32**, 215–255 (2004).
16. Brown, E. T., Stallard, R. F., Larsen, M. C., Raisbeck, G. M. & Yiou, F. Denudation rates determined from the accumulation of in-situ produced [10]Be in the Luquillo Experimental Forest, Puerto Rico. *Earth Planet. Sci. Lett.* **129**, 193–202 (1995).
17. Riebe, C. S., Kirchner, J. W., Granger, D. E. & Finkel, R. C. Erosional equilibrium and disequilibrium in the Sierra Nevada, inferred from cosmogenic [26]Al and [10]Be in alluvial sediment. *Geology* **28**, 803–806 (2000).
18. Schaller, M., von Blanckenburg, F., Hovius, N. & Kubik, P. W. Large-scale erosion rates from in-situ produced cosmogenic nuclides in European river sediments. *Earth Planet. Sci. Lett.* **188**, 441–458 (2001).
19. Vance, D., Bickle, M., Ivy-Ochs, S. & Kubik, P. W. Erosion and exhumation in the Himalaya from cosmogenic isotope inventories in river sediments. *Earth Planet. Sci. Lett.* **206**, 273–288 (2003).
20. Burbank, D. W. *et al.* Bedrock incision, rock uplift and threshold hillslopes in the northwestern Himalayas. *Nature* **379**, 505–510 (1996).
21. Roering, J. J., Kirchner, J. W. & Dietrich, W. E. Hillslope evolution by nonlinear, slope-dependent transport: steady state morphology and equilibrium adjustment timescales. *J. Geophys. Res.* **106**, 16499–16513 (2001).
22. Bierman, P. & Steig, E. Estimating rates of denudation using cosmogenic isotope abundances in sediment. *Earth Surf. Processes Landforms* **21**, 125–139 (1996).
23. Granger, D. E., Kirchner, J. W. & Finkel, R. Spatially averaged long-term erosion rates measured from in situ-produced cosmogenic nuclides in alluvial sediment. *J. Geol.* **104**, 249–257 (1996).
24. Niemi, N. A., Oskin, M. E. & Burbank, D. A numerical simulation of the effects of mass-wasting on cosmogenically determined erosion rates. *Eos* **85** (Fall Meet. Suppl.), Abstract H51C–1157 (2004).
25. Putkonen, J. Continuous snow and rain data at 500 to 4400 m altitude near Annapurna, Nepal, 1999–2001. *Arct. Antarct. Alpine Res.* **36**, 244–248 (2004).
26. Beaumont, C., Jamieson, R. A., Nguyen, M. H. & Lee, B. Himalayan tectonics explained by extrusion of a low-viscosity crustal channel coupled to focused surface denudation. *Nature* **414**, 738–742 (2001).
27. Hodges, K. V., Hurtado, J. M. & Whipple, K. X. Southward extrusion of Tibetan crust and its effect on Himalayan tectonics. *Tectonics* **20**, 799–809 (2001).

....

Geobiology of a microbial endolithic community in the Yellowstone geothermal environment

Jeffrey J. Walker, John R. Spear & Norman R. Pace

Department of Molecular, Cellular and Developmental Biology and the Center for Astrobiology, University of Colorado, Boulder, Colorado 80309-0347, USA

....

The endolithic environment, the pore space of rocks, is a ubiquitous habitat for microorganisms on the Earth[1] and is an important target of the search for life elsewhere in the Solar System[2]. Photosynthetic, endolithic microbial communities commonly inhabit the outer millimetres to centimetres of all rocks exposed to the Earth's surface. In the most extreme terrestrial climates, such as hot and cold deserts, endolithic microorganisms are often the main form of life[3–5]. The endolithic microhabitat

gives protection from intense solar radiation and desiccation, and it provides mineral nutrients, rock moisture and growth surfaces[4,5]. Here we describe the discovery and identification of the constituents of an extremely acidic (pH 1) endolithic microbial community inhabiting the pore space of rocks in the geothermal environment of Yellowstone National Park, USA. Subjected to silica mineralization, such endolithic communities constitute biomarkers that can become fossilized and potentially preserved in the geological record. Remnants of these communities could serve as biosignatures and provide important clues about ancient life associated with geothermal environments on the Earth or elsewhere in the Solar System.

Lush and unusual photosynthetic communities inhabit silica rocks in Yellowstone's Norris Geyser Basin. These rocks are primarily chalcedonic sinters and are warmed to ~35 °C by subsurface geothermal activity. The stark, weathered surfaces of these exposed rocks show no evidence of the rich life hidden beneath the surface (Fig. 1). Fractured rock samples show clear signs of photosynthetic endolithic communities, which inhabit a distinct green band from 1 to 15 mm thick and 2–10 mm beneath the surface exposed to light. Photosynthetic pigments, primarily chlorophyll of red algae (see below), impart a green colour. Although endolithic growth of red algae is known in other volcanic areas[6], this is the first comprehensive molecular analysis of the microbial diversity and composition of these unique communities and their potential mineralization and fossilization.

Pore waters extracted from the rock had a pH of ~1 and contained high concentrations of sulphuric acid, metals and silicates (for example 1,343 p.p.m. SO_4, 8,893 p.p.m. Al, 983 p.p.m. Mn, 551 p.p.m. Cu, 1,038 p.p.m. As, 102 p.p.m. Fe and 166 p.p.m. SiO_2). The acidity is a product of the physical and biological oxidation of reduced sulphur species to sulphuric acid[7,8]. Rocks that harboured endolithic communities contained 10–32% pore water by weight. The evaporation of pore water concentrates dissolved species, particularly silica, which precipitates and encrusts the microbial community as it grows. Similar mineralization processes are observed in living microbial communities directly associated with terrestrial[2,9–11] and marine[12] thermal springs. The processes that fossilize microbial communities, how these fossils are preserved in the geological record, and their potential as biosignatures have been examined extensively[2,9,13–16]. The community described here is a unique opportunity to observe an endolithic microbial community in the process of fossilization.

To understand the kinds of organism that constitute this previously unknown community, we used DNA sequence-based methods that rely on genomic DNA extracted directly from the environment instead of cultivation techniques that typically grow much less than 1% of the organisms present[17]. We isolated total community DNA from rock samples and used this as a template to amplify by polymerase chain reaction (PCR) small-subunit ribosomal RNA genes representative of organisms present in the community. We used universal PCR primers that target all three domains of life, the Bacteria, Archaea and Eukarya, as well as primers that target only the Bacteria. Individual PCR-amplified rRNA genes were cloned and segregated into libraries, collections of 96 randomly selected rRNA gene clones. In total, we screened and analysed 864 clones, of which we sequenced 342. Results (Fig. 2a) show that the community is relatively simple, composed mainly of organisms with rRNA gene sequences of ~40 species-level relatedness groups (at least 97% rRNA sequence identity), a conservative estimate of species-level diversity based on rRNA sequence variation[18].

Two kinds of sequence dominated the clone libraries. About 26% of clones (225 of 864) were most closely related by phylogenetic analysis (98–99% sequence identity) to chloroplast rRNA genes of *Cyanidium caldarium*, an acidophilic eukaryotic red alga. This indicates that closely related *Cyanidium* species might be the
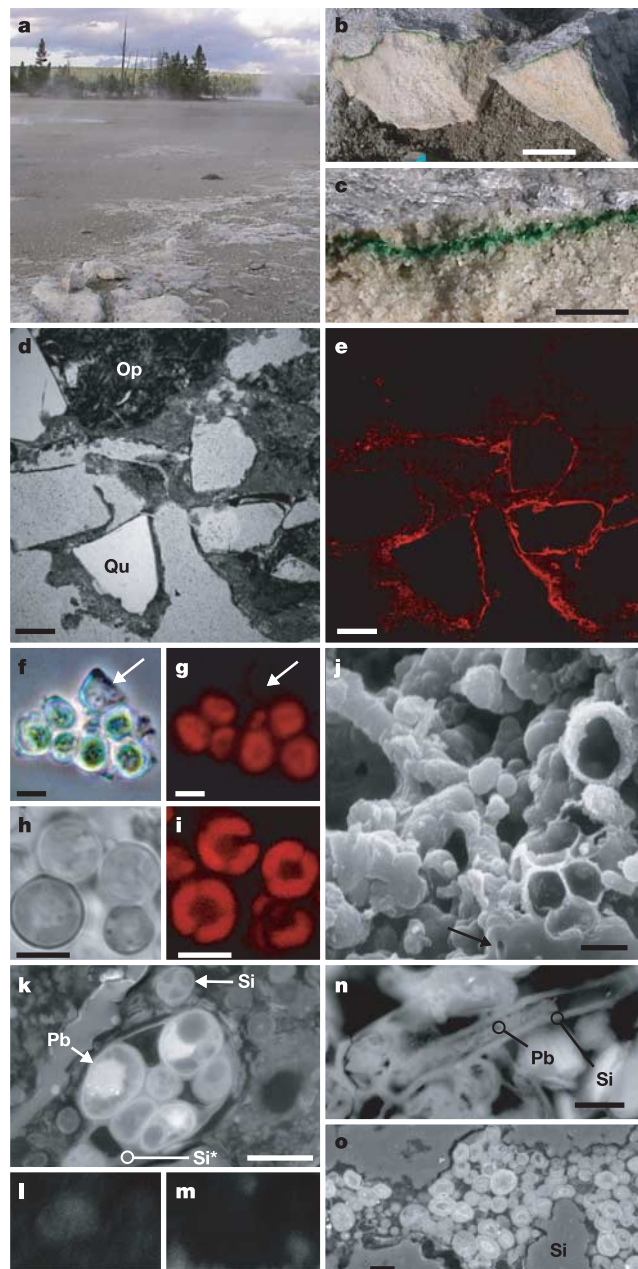

Figure 1 Endolithic microbial communities in highly acidic (pH1) chalcedonic sinters of Yellowstone's Norris Geyser Basin. **a**, Outcrops harbouring cryptoendoliths (foreground). **b**, **c**, Fractured sinter reveals distinct green layer of photosynthetic microbial life. Scale bars, 5 cm (**b**) and 1 cm (**c**). **d**, **e**, LSCM images of 30-μm petrographic thin section of endolithic community. **d**, Transmitted light shows that host rock is chalcedonic sinter with quartz grains (Qu) cemented by microcrystalline opaline silica (Op). **e**, Fluorescence associated with cells containing chlorophyll imaged with LSCM (excitation at 488 nm, detection at 630–650 nm). Scale bars, 200 μm. **f**, **g**, Micrographs of *Cyanidium* spp. encrusted in mineral casts. Transmitted light (**f**) shows casts with and without (arrows) fluorescent *Cyanidium* spp. cells (**g**). Scale bars, 5 μm. **h**, **i**, LSCM micrographs of *Cyanidium* spp. cultivated in enrichments imaged with transmitted light (**h**) and fluorescence (**i**) as in **e**. Scale bars, 5 μm. **j**, SEM image of broken spherical silica casts that form around individual *Cyanidium* spp. cells and a tubular cast (arrow) that forms around a network of cells presumed to be largely *Mycobacterium* spp. Scale bar, 5 μm. **k–m**, BSE–SEM image (**k**) and EDS maps (**l**, **m**) of transverse section of presumed *Cyanidium* spp. cellular structures. Si*, EDS point spectra. Heavy metals stain biological material (Pb) (**l**). One cellular structure (Si) did not stain with Pb and had a strong Si signal (**m**). Scale bar, 5 μm. **n**, BSE–SEM image of tubular structure. EDS point spectrum showed that the cast (Si) was primarily silicon and that the inner material (Pb) was stained with lead. Scale bar, 5 μm. **o**, BSE–SEM image of cells in pore space surrounded by silica cement (Si). Scale bar, 5 μm.

main primary producers of the community. *Cyanidium* and other undetected genera of the Cyanidiaceae family, *Cyanidioschyzon* and *Galdieria*, are the most acid-tolerant photosynthetic organisms known. Nuclear rRNA genes of *Cyanidium* spp. were detected in enrichment cultures of *Cyanidium* spp. but not in universal community libraries. Analysis of photosynthetic pigments extracted directly from the community showed only chlorophyll *a* and other associated photosynthetic pigments identical with those in *Cyanidium* species cultured from Norris Geyser Basin (see Methods).

The most abundant group of rRNA gene clones analysed, a remarkable 37% of the total (328 of 864), were previously unidentified *Mycobacterium* species, members of the bacterial division Actinobacteria (Fig. 2b). Enrichments were not successful in the cultivation of *Mycobacterium* spp., as assayed by rRNA probe hybridization. Famous as pathogens, mycobacteria cause diseases such as tuberculosis and leprosy in humans. Mycobacteria also are considered common constituents of environmental settings such as soil and freshwater habitats, but they have not previously been encountered as such a large component of an environmental

Figure 2 Microbial diversity of the Norris community. **a**, Phylogenetic distribution of rRNA gene sequences amplified from the Norris community (*n* = 864). **b**, Composite tree diagram of the phylogenetic relationship of endolithic community rRNA gene sequences (represented by solid wedge) to those of known *Mycobacterium* spp. (expanded portion of tree) and the relationship of the mycobacteria group to other groups (open wedges) of the bacterial division Actinobacteria. Phylogenetic analyses showed that rDNA sequences from the Norris community formed a distinct group of mycobacteria supported in all analyses (minimum evolution, maximum parsimony and maximum likelihood) with strong statistical support (>70% bootstrap value). The Norris sequences are most closely related to *M. elephantis* (~97%), and the association of the *M. elephantis* group as a sister species to the Norris group was present in all trees in all analyses and was supported statistically by maximum evolution bootstrap analysis but not by the other methods.

microbial community. Such organisms typically are of low abundance (much less than 1%) and detected in the environment only with specific and sensitive assays[19]. The role of mycobacteria in these natural settings is not well understood but is generally considered heterotrophic. Environmental mycobacteria can adapt to acidic environments. Studies of environmental soils and sediments with quantitative cultures show an enrichment of mycobacteria at low pH. The richest mycobacterial environment previously reported (~1% of the community) is a mildly acidic (pH 4) forest soil[19]. Mycobacteria have not been encountered previously in such highly acidic (pH 1) volcanic environments as those reported here.

Although the primary energy source for the community is probably photosynthesis, the flux of geochemical species through the habitat indicates that lithotrophy, the metabolism of reduced inorganic compounds for energy, might contribute to the overall energy budget of the community. Dissolved species that could potentially serve as fuels include metals, sulphur compounds and hydrogen, an important energy source for microbes abundant in Norris Geyser Basin[20]. The most diverse group of rRNA gene sequences in the community represented ~14 distinct groups of the bacterial division Proteobacteria and comprised ~11% of the total clones. Most of these sequences (~9%) belong to the γ-Proteobacteria, a group that includes lithotrophic organisms that metabolize hydrogen and sulphide. In addition, rRNA gene sequences closely related (99% identity) to those of two known lithoautotrophs, *Sulfobacillus disulfidooxidans* and *Leptospirillum ferrooxidans*, each comprised ~1% of the community. Only ~5% of clones were representative of members of the domain Archaea, which are popularly associated with such 'extreme' geothermal environments; however, bacteria, and to some extent eukaryotes, are equally important in these settings[17].

We used several imaging techniques to investigate the physical structure of the community. Light microscopy of petrographic thin sections showed the rock to be a chalcedonic sinter with large, weathered, quartz grains cemented by opaline silica (Fig. 1d). To determine the distribution of photosynthetic organisms *in situ*, we imaged the fluorescence associated with chlorophyll in thin sections. Fluorescence localized to the microcrystalline cement and was most intense along quartz grain margins (Fig. 1e). Individual cells were observed at higher magnifications, although the fluorescence of cells embedded in the mineral matrix was highly scattered. Images of *Cyanidium* cells in freshly disrupted samples showed that many apparently healthy cells were encrusted in a crystalline matrix, presumably silica (Fig. 1f, g). Spectral analysis of fluorescence in thin sections and that of individual *Cyanidium* spp. cells yielded identical results.

Field-emission scanning electron microscopy (SEM) revealed a complex fabric of mineralized filamentous and spherical casts (Fig. 1j) in the pigmented zone of colonization. Nearly identical mineralized silica biofabrics occur in living microbial mats (nominally *Cyanidium caldarium*) in acidic (pH 2) thermal springs in Hokkaido, Japan[10]. Similar fabrics are also observed in mineralized and recently fossilized microbial communities in other thermal spring environments[2,9,11,12]. Recent findings indicate that fossilized subsurface biofabrics might be preserved in the geological record[2]. We imaged sections of resin-embedded endolithic community with backscattered-electron-imaging scanning electron microscopy (BSE–SEM), which showed spherical and filamentous cellular structures embedded in the mineral matrix (Fig. 1k–m). Samples were treated with heavy metals (osmium, lead and uranium), which stain and give contrast to biological materials in BSE–SEM images. The spherical cellular structures had outer diameters of 3.5–6.6 μm (average 5.0 ± 0.8 μm, *n* = 50), similar to the size of *Cyanidium* cells we observed by light microscopy. We analysed the elemental composition of samples with energy-dispersive X-ray spectroscopy (EDS). The interiors of most cellular structures had strong signals
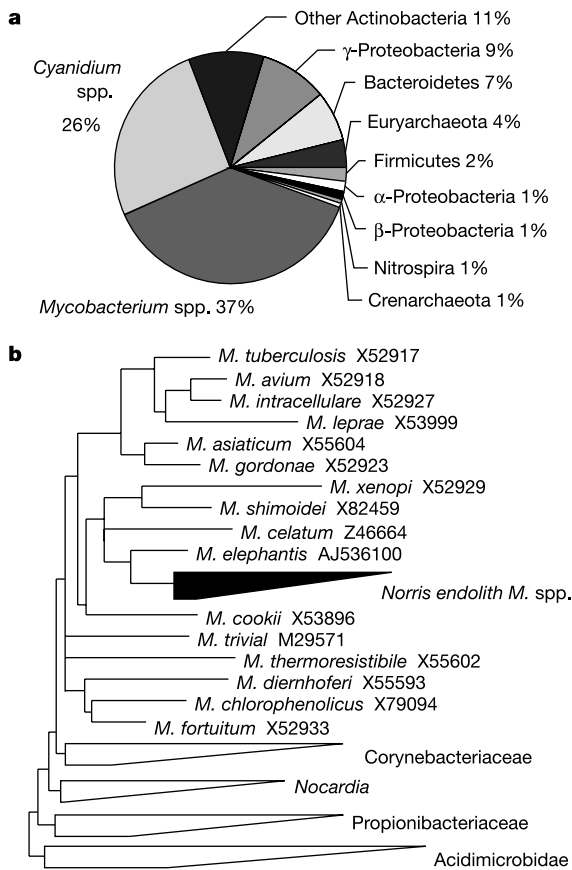
for lead, osmium and uranium, whereas the signal from the surrounding material indicated primarily silicon (Fig. 1k). Some cellular structures did not stain and had strong silicon signals, which indicates that they might already have been mineralized and could become fossilized.

The abundance of mycobacterial clones (~37%) detected in the community leads us to postulate that the ubiquitous curvilinear filamentous casts observed formed around a biofabric of primarily mycobacteria, although other organisms detected are probably also involved. Mycobacteria are known to form complex filamentous and branched biofilms[21]. The filaments in this study have a tubular construction with inner diameters of 0.8–3.0 μm (average 1.9 ± 0.5 μm, $n = 60$), typical of bacterial cells. BSE–SEM imaging showed that the filamentous structures are segmented, and EDS analysis indicates that the interiors contain biological material and that the casts are primarily silica (Fig. 1m). Similar filamentous structures observed in specimens collected from silica-depositing thermal springs in Yellowstone have been shown to be fossilized filament casts of microbes[9].

Mineralization of endolithic communities associated with geothermal environments might lead to the preservation of identifiable biosignatures. Fossils of endolithic microbial communities recently discovered in Antarctic sandstone preserve exquisite detail of the internal structures of cells[22]. We expect that the abundance of Yellowstone endolithic communities in environments favourable to mineralization leads to their preservation in the geological record. Unequivocal microfossils from the 2.0-Gyr-old Gunflint formation (Ontario, Canada) were formed by silica mineralization in an environment interpreted as analogous to that in Yellowstone[23,24], although the exact nature of that environment remains uncertain. Regardless of the environment, Gunflint microfossils demonstrate the potential for microfossils to form in siliceous environments and to persist in the Earth's geological record for a minimum of 2 Gyr.

Mineralized endolithic communities such as those described here could be a highly diagnostic indicator of past life on Mars. Evidence of past geothermal activity on Mars includes volcanism and possible hydrothermal systems, which could be analogous to those of Yellowstone[14,25]. Missions to Mars target such areas in the search for evidence of life, past or present, on Mars. The endolith is a critical habitat to explore in that search. The rich diversity of endolithic life in the geothermal environment of Yellowstone, combined with the potential for biosignature preservation, indicates that rocks associated with former hydrothermal systems might be the best hope for finding evidence of past life on the martian surface. □

Methods

Sample description
Samples were collected from outcrops located in Norris Geyser Basin, Yellowstone National Park, USA. The community described was collected from a single site (44° 43.92′ N, 110° 42.63′ W).

Chemical analysis
Rock pH was measured as described[26]. Pore water was extracted by centrifugation for standard chemical analysis by inductively coupled plasma (ICP)–atomic absorption spectrometry, ICP–mass spectrometry and ion chromatography as described[20].

Molecular community analysis
Molecular phylogenetic community rRNA analysis was performed with DNA extracted from crushed rock samples as described[20]. The average yield of extracted DNA was 3.1 mg of DNA per gram of crushed rock. PCR primers used in this study were 27F, 515F and 1391R. In situ hybridizations for mycobacterial species were performed as described[27].

Microscopy
Petrographic thin sections were prepared from resin-embedded samples and imaged with light and laser-scanning confocal microscopy (LSCM) as described[28]. Conventional SEM specimens were fixed in 4% glutaraldehyde, critical-point dried and coated with gold[13]. BSE–SEM was performed as described[22,29] with an FEI Quanta 600 SEM, BSE detector and Princeton Gamma Tech EDS system.

Photosynthetic pigment analysis
Photosynthetic pigments extracted from rock samples were analysed as described[30]. Strains of *Cyanidium* spp. cultured from Norris Geyser Basin for comparison were obtained from the Culture Collection of Microorganisms from Extreme Environments (CCMEE) and included strains NC-5-Cl-1 CCMEE 5584 and C-Cl-1 CCMEE 5564.

1. Golubic, S., Friedmann, E. I. & Schneider, J. The lithobiontic ecological niche, with special reference to microorganisms. *J. Sedim. Petrol.* **51,** 475–478 (1981).
2. Hofmann, B. A. & Farmer, J. D. Filamentous fabrics in low-temperature mineral assemblages: are they fossil biomarkers? Implications for the search for a subsurface fossil record on the early Earth and Mars. *Planet. Space Sci.* **48,** 1077–1086 (2000).
3. Friedmann, E. I. & Ocampo, R. Endolithic blue-green algae in dry valleys—primary producers in Antarctic desert ecosystem. *Science* **193,** 1247–1249 (1976).
4. Friedmann, E. I. Endolithic microorganisms in the Antarctic cold desert. *Science* **215,** 1045–1053 (1982).
5. Bell, R. A. Cryptoendolithic algae of hot semiarid lands and deserts. *J. Phycol.* **29,** 133–139 (1993).
6. Gross, W., Kuver, J., Tischendorf, G., Bouchaala, N. & Busch, W. Cryptoendolithic growth of the red alga *Galdieria sulphuraria* in volcanic areas. *Eur. J. Phycol.* **33,** 25–31 (1998).
7. Mosser, J. L., Misser, A. G. & Brock, T. D. Bacterial origin of sulfuric acid in geothermal habitats. *Science* **179,** 1323–1324 (1973).
8. White, D. E., Hutchinson, R. A. & Keith, T. E. C. *The Geology and Remarkable Thermal Activity of Norris Geyser Basin, Yellowstone National Park, Wyoming.* (US Geol. Surv. Professional Paper no. 1456, Washington DC, 1988).
9. Cady, S. L. & Farmer, J. D. in *Evolution of Hydrothermal Ecosystems on Earth (and Mars?)* (eds Bock, G. R. & Goode, J. A.) 150–173 (Wiley, New York, 1996).
10. Asada, R. & Tazaki, K. Silica biomineralization of unicellular microbes under strongly acidic conditions. *Can. Mineral.* **39,** 1–16 (2001).
11. Blank, C. E., Cady, S. L. & Pace, N. R. Microbial composition of near-boiling silica-depositing thermal springs throughout Yellowstone National Park. *Appl. Environ. Microbiol.* **68,** 5123–5135 (2002).
12. Zierenberg, R. A. & Schiffman, P. Microbial control of silver mineralization at a sea-floor hydrothermal site on the northern Gorda Ridge. *Nature* **348,** 155–157 (1990).
13. Cady, S. L., Farmer, J. D., Grotzinger, J. P., Schopf, J. W. & Steele, A. Morphological biosignatures and the search for life on Mars. *Astrobiology* **3,** 351–368 (2003).
14. Farmer, J. D. & Des Marais, D. J. Exploring for a record of ancient Martian life. *J. Geophys. Res. Planets* **104,** 26977–26995 (1999).
15. Banfield, J. F., Moreau, J. W., Chan, C. S., Welch, S. A. & Little, B. Mineralogical biosignatures and the search for life on Mars. *Astrobiology* **1,** 447–465 (2001).
16. Des Marais, D. J. & Walter, M. R. Astrobiology: Exploring the origins, evolution, and distribution of life in the Universe. *Annu. Rev. Ecol. Syst.* **30,** 397–420 (1999).
17. Pace, N. R. A molecular view of microbial diversity and the biosphere. *Science* **276,** 734–740 (1997).
18. Stackebrandt, E. & Goebel, B. M. Taxonomic note: A place for DNA-DNA reassociation and 16S rRNA sequence analysis in the present species definition in bacteriology. *Int. J. Syst. Bacteriol.* **44,** 846–849 (1994).
19. Iivanainen, E. K., Martikainen, P. J., Raisanen, M. L. & Katila, M. L. Mycobacteria in boreal coniferous forest soils. *FEMS Microbiol. Ecol.* **23,** 325–332 (1997).
20. Spear, J. R., Walker, J. J., McCullem, T. M. & Pace, N. R. Hydrogen and bioenergetics in the Yellowstone geothermal ecosystem. *Proc. Natl Acad. Sci. USA* **102,** 2555–2560 (2005).
21. Hall-Stoodley, L. & Lappin-Scott, H. Biofilm formation by the rapidly growing mycobacterial species *Mycobacterium fortuitum. FEMS Microbiol. Lett.* **168,** 77–84 (1998).
22. Ascaso, C. & Wierzchos, J. The search for biomarkers and microbial fossils in Antarctic rock microhabitats. *Geomicrobiol. J.* **20,** 439–450 (2003).
23. Schopf, J. W., Barghoorn, E. S., Maser, M. D. & Gordon, R. O. Electron microscopy of fossil bacteria two billion years old. *Science* **149,** 1365–1367 (1965).
24. Walter, M. R. A hot spring analog for the depositional environment of Precambrian iron formations of the Lake Superior Region. *Econ. Geol.* **67,** 965–980 (1972).
25. Christensen, P. R. *et al.* Morphology and composition of the surface of Mars: Mars Odyssey THEMIS results. *Science* **300,** 2056–2061 (2003).
26. Doemel, W. N. & Brock, T. D. pH of very acid soils. *Nature* **229,** 574 (1971).
27. St. Amand, A. L., Frank, D. N., De Groote, M. A. & Pace, N. R. Microscopic detection of *Myocbacterium avium* complex organisms in tissue with specific rRNA oligonucleotide probes. *J. Clin. Microbiol.* **4**(43), (in the press).
28. Papineau, D., Walker, J. J., Mojzsis, S. J. & Pace, N. R. Composition and structure of microbial communities from stromatolites of Hamelin Pool in Shark Bay, Western Australia. *Appl. Environ. Microbiol.* (in the press).
29. Wierzchos, J. & Ascaso, C. Application of backscattered electron imaging to the study of the lichen rock interface. *J. Microsc.* **175,** 54–59 (1994).
30. Frigaard, N. U., Larsen, K. L. & Cox, R. P. Spectrochromatography of photosynthetic pigments as a fingerprinting technique for microbial phototrophs. *FEMS Microbiol. Ecol.* **20,** 69–77 (1996).